

Inverted open microwells for single-cell trapping, cell-cell interaction analysis and live cell functional sorting

Massimo Bocchi, Laura Rambelli, Andrea Faenza, Luca Giulianelli, Nicola Pecorari, Enri Duqi, and Roberto Guerrieri

Electronic Supporting Information

1. Models for DEP and trans-membrane potential calculation

For calculations of forces acting on cells we considered a membrane specific capacitance $C_m=9.7\text{mF/m}^2$, a cytoplasm resistivity $\rho_c=3.57\Omega\text{m}$, a membrane resistivity $\rho_m=0.6\Omega\text{m}$ and a cell radius of $9\mu\text{m}$, according to typical values found in the literature for K562 cells¹.

1.1 Dielectrophoresis

All DEP simulations were performed by considering a single-shell model for the cell. The Clausius-Mossotti factor was calculated according to the theory described by Huang et al.². With the parameters indicated above and for a physiological medium having a conductivity of 1.5 S/m and a relative permittivity of 78.5, the real part of the Clausius-Mossotti (f_{CM}) factor has the spectrum shown in Fig. S1. We observe that, being the sign always negative in the frequency range shown in the figure, the cell is always subjected to a negative DEP force. In particular, for a frequency of the applied signal of 100 kHz, as the one adopted in our experiments, the value of the f_{CM} factor is close to its minimum value of -0.5. Hence, this frequency represents the optimal condition for cell manipulation through negative DEP.

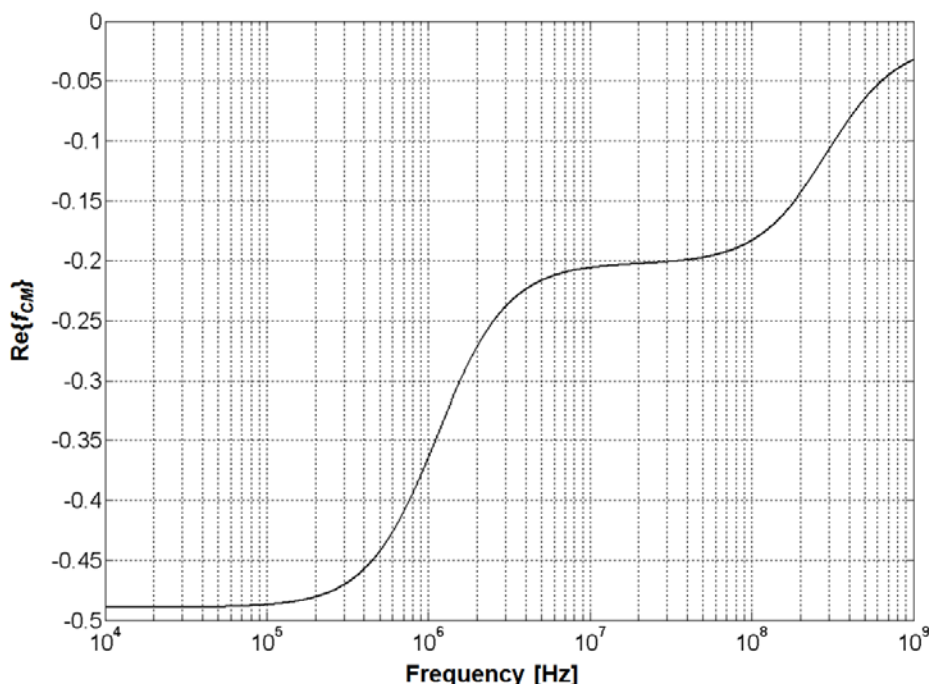


Fig. S1 Real part of the Clausius-Mossotti factor as a function of the frequency of the applied signal for a cell suspended in physiological medium.

1.2 Trans-membrane potential

To determine the maximum trans-membrane potential experienced by cells manipulated by DEP in the inverted open microwell, we identified the worst case condition for the cell and applied the model described by equations (10) and (11) in the main text of the paper. Two possible electric field configurations (BLOCK and LOAD) can be activated in the microwell, with a typical amplitude of the signal applied to the electrodes of 1.2 V and 0.6 V, respectively. The trans-membrane potential exerted on a cell depends on its position in the microstructure along the vertical microwell axis where the cell result to be trapped (Fig. S2). In BLOCK mode, the cell is trapped at the microwell entrance at a height of $8\mu\text{m}$

above the microwell, as shown in Fig. 7 of the main article. Considering a radius of 9 μm , the cell boundary reaches the level of -1 μm , where the trans-membrane potential has a value of 109 mV. This represents the worst case condition in BLOCK mode. For the LOAD mode, the cell travels along the microwell axis and experiences a maximum trans-membrane potential of 101 mV at a height of -32 μm . In conclusion the maximum trans-membrane potential is the one experienced in BLOCK mode which is below the value of 200 mV, considered as the safety limit for not inducing adverse effects on the cell³.

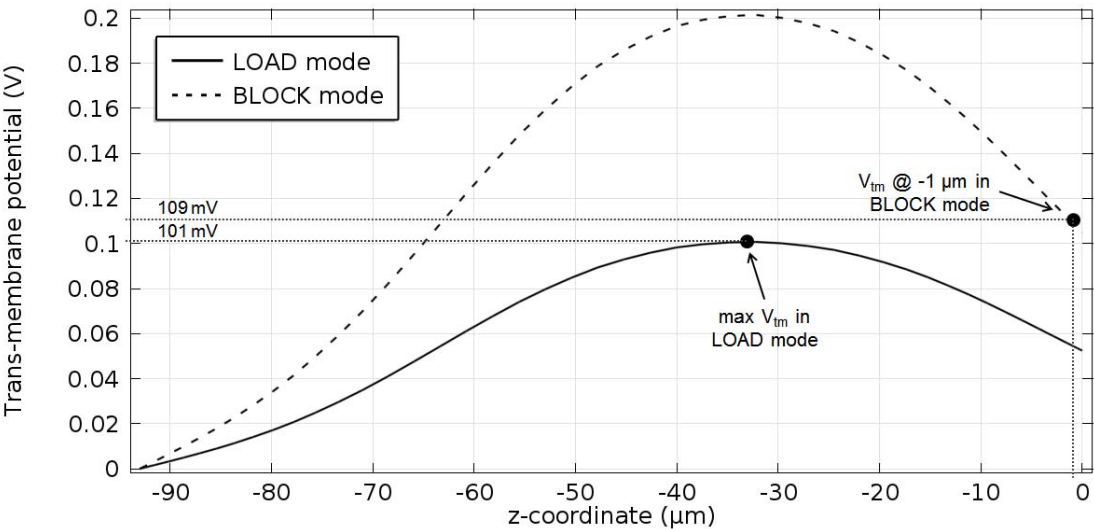


Fig. S2 Plot of the trans-membrane potential along the microwell axis for BLOCK and LOAD configurations, featuring a value of the voltage amplitude between the electrodes of 0.6 V and 1.2 V, respectively. The level of 0 μm corresponds to the microwell top.

2. Heat transfer simulations

Joule heating generated by the alternating electric field in physiological medium was simulated on a 3D structure comprising a single microwell and a substrate tile having an area of 4.5 mm x 4.5 mm, as shown in Fig. S3A, so that the distance between the microwell and each of the boundaries is equal to half the pitch between the microwells. In this situation a symmetry condition with no heat flux along the lateral boundaries was set, as the selected tile is surrounded by other tiles where the same heat flux is generated. Hence, the only possible heat exchange occurs through the top and bottom sides of the device, that are exposed to the external environment. We modeled these two boundaries assuming the heat to be exchanged by natural convection using the equation (9) in the main article, where the external environment is represented by air at an ambient temperature of 25°C. The properties of the materials used in the simulation are reported in Table S1.

Table S1 Properties of materials used in heat transfer simulations

Layer	Material	Layer thickness [μm]	Heat capacity [J/(kg·K)]	Thermal conductivity [J/(m·K)]
Liquid	Water	150	4182	0.6
Top cover	PMMA	750	1420	0.19
Top adhesive	Silicone	50	1690	0.13
Substrate	Polyimide	93	1100	0.15
Metal wires	Copper	9	385	400

Simulation results for the worst case condition (BLOCK mode), featuring a voltage amplitude of 1.2 V, are shown in Fig. S3B. The maximum temperature increase is limited to 0.7°C and is concentrated at the center of the microwell between the two electrodes. At the bottom side the temperature increase is about 0.5°C.

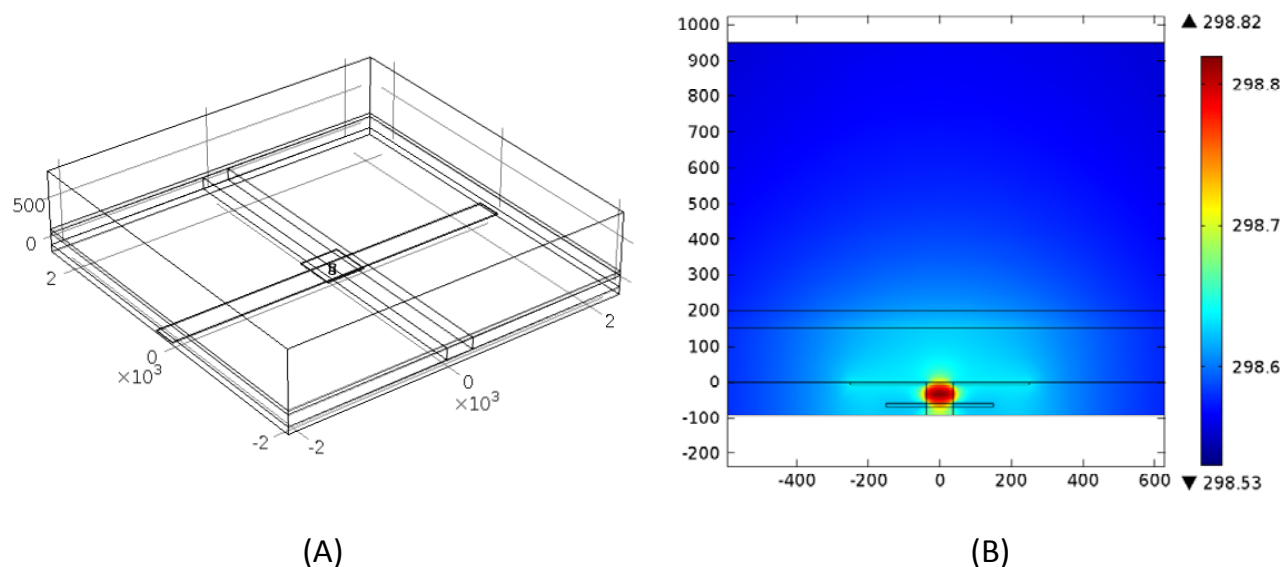


Fig. S3 (A) 3D representation of the structure designed for heat transfer simulations. (B) Slice plot on a vertical cross section along the microwell axis of the temperature distribution in the device.

3. Fluid mixing simulations

Fluid mixing simulations were performed in the microwell to study the possible undesired effect of a lateral flow acting on cells trapped at the air-fluid interface and potentially dislodging them from the central position. This effect results to be higher if the ratio between the microwell diameter and height increases. Fig. S4 shows the results of a simulation performed on a microwell with a diameter of 75 μm and different heights. For a height of 93 μm (Prototype 1) the lateral flow in the lower part of the microwell is relatively high and reaches a velocity of about 6.5 $\mu\text{m}/\text{sec}$ at a vertical distance of 20 μm from the air-fluid interface. Hence, under these conditions, cells are dislodged by the lateral flow, as confirmed by experiments on Prototype 1. For deeper microwells, this effect is rapidly reduced. Experiments on Prototype 2, featuring a height of 143 μm , did not show any cell movement upon fluid flow activation after cell trapping on the air-fluid interface.

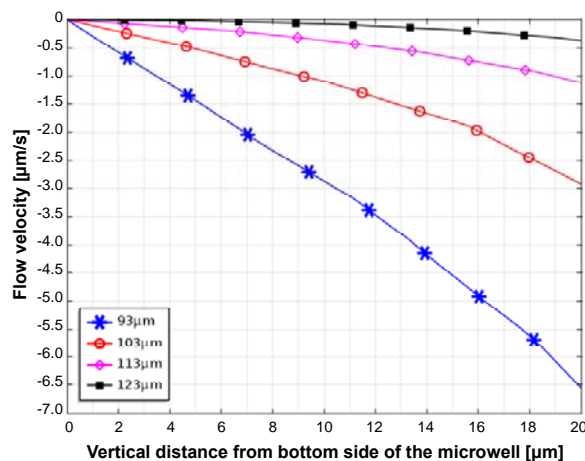


Fig. S4 Horizontal component of the flow velocity in the microwell as a function of the distance from the bottom side of the microwell along the vertical axis. Results are reported from simulation of four different microwell depths for a microwell diameter of 75 μm and an average flow velocity of 2.54 mm/s in the microchannel. Negative values indicate a flow in the opposite direction to the flow in the microchannel.

References

1. F. H. Labeed, H. M. Coley, and M. P. Hughes, *Biochimica et Biophysica Acta (BBA) - General Subjects*, 2006, **1760**, 922-929.
2. Y. Huang, R. Holzel, R. Pethig, and X.-B. Wang, *Physics in Medicine and Biology*, 1992, **37**, 1499-1517.
3. N. Mittal, A. Rosenthal, and J. Voldman, *Lab Chip*, 2007, **7**, 1146-1153.